UFSM

CIÊNCIA e NATURA

ISSN 2179-460X
OPEN ACCESS

Ci. e Nat., Santa Maria, v. 47, n. spe. 3, e84042, 2025, • https://doi.org/10.5902/2179460X84042
Submitted: 10/06/2023 • Approved: 03/12/2024 • Published: 30/04/2025

IX Encontro Sul Brasileiro de Meteorologia

Wavelet analysis applied to CO_2 fluxes in native grasslands of the Pampa biome under the influence of different ENSO phenomena

Análise Wavelet aplicada aos fluxos de CO_2 em pastagem nativa do bioma Pampa sob influência de diferentes fenômenos ENOS

João Antonio Voltz da Silva[I], Débora Regina Roberti[I], Benno August Ludwig Bodmann[I], Richard Reno da Costa Lobato[I], Alecsander Mergen[I]

[I] Universidade Federal de Santa Maria, Santa Maria, RS, Brasil

ABSTRACT

The Brazilian Pampa biome is recognized for its extensive area dedicated to livestock farming, being one of the main producers of beef in the country. Greenhouse gas emissions or absorptions, such as CO_2, are influenced by periods associated with ENSO phenomena (El Niño, EL and La Niña, LN). Continuous and Cross Wavelet transform analyses are effective methods for investigating differences in the gas exchanges, allowing the examination of temporal CO_2 variability and the relationship with meteorological variables at different time scales. The meteorological and CO_2 flux data used in this analysis were collected from a flux tower at the Santa Maria experimental site, with CO_2 fluxes obtained using the Eddy Covariance technique. Wavelet analyses demonstrated the ability to identify flux patterns across different temporal scales, considering the influence of distinct phases of the ENSO in the Brazilian Pampa biome. The results indicate that the main differences between the EL and LN phenomena occur on a time scale between 16 to 32 days in the relationship of CO_2 flux and Precipitation, being in spring for EL and summer/autumn in LN. The observed temporal patterns of CO_2 fluxes and environmental variables highlight the importance of modeling CO_2 flux concerning meteorological trends.

Keywords: CWT; XWT; Eddy covariance; Surface fluxes; El Niño; La Niña

RESUMO

O bioma Pampa brasileiro é reconhecido por sua extensa área dedicada à pecuária, sendo um dos principais produtores de carne bovina do país. As emissões ou absorções de gases de efeito estufa, como o CO_2, são influenciadas por períodos associados aos fenômenos ENOS (El Niño, EL, e La Niña, LN).

Análises de transformada wavelet contínua e cruzada são métodos eficazes para investigar diferenças nas trocas gasosas, permitindo o exame de variações temporais de CO_2 e sua relação com variáveis meteorológicas em diferentes escalas de tempo. Os dados meteorológicos e de fluxo de CO_2 usados nesta análise foram coletados de uma torre de fluxo no sítio experimental de Santa Maria, com fluxos de CO_2 obtidos usando a técnica de covariância dos vórtices. As análises de wavelet demonstraram a capacidade de identificar padrões de fluxo em diferentes escalas temporais, considerando a influência de fases distintas do ENSO no bioma Pampa brasileiro. Os resultados indicam que as principais diferenças entre os fenômenos EL e LA ocorrem em uma escala de tempo entre 16 a 32 dias na relação de fluxo de CO_2 e Precipitação, sendo na primavera para EL e verão/outono em LN. Os padrões temporais observados de fluxos de CO_2 e variáveis ambientais destacam a importância da modelagem do fluxo de CO_2 em relação às tendências meteorológicas.

Palavras-chave: CWT; XWT; Covariância dos vórtices; Fluxos superficiais; La Niña; El Niño

1 INTRODUCTION

The Brazilian Pampa biome represents currently about 62.2% of the entire territory of Rio Grande do Sul (Boldrini, 2010) and has great economic importance since Colonial Brazil. Livestock farming gained prominence in the region when Portugal saw the Pampa as an opportunity to supply other Brazilian regions with meat (Reichert and Schumacher, 2015, Roesch et al., 2009). However, over the years, concerns about global warming and the effects of greenhouse gases (GHG) have increased the interest in more productive and environmentally friendly management practices (Herzog et al., 2000; Popp et al., 2010). These practices must be adapted to the different climatic phenomena that routinely occur in the region and to the imminent climate change that has intensified extreme events globally. In this context, identifying patterns related to carbon exchanges between the ecosystem and the atmosphere is crucial for ensuring that future adaptations can be implemented efficiently.

The Brazilian Pampa biome is predominantly influenced by key climatic phenomena, including La Niña (LN) and El Niño (EN), which are phases of the El Niño Southern Oscillation (ENSO) phenomenon (Schossler et al., 2018; Lobato, 2022). The EN phase typically results in above-average precipitation in this region, while LN leads to below-average rainfall, which has intensified due to climate change. Although the effects of these phenomena on the Pampa biome may be less noticeable in the short term compared to agriculture, it is crucial to understand how the biome's vegetation, primarily composed of C4 and C3 grasses responds during drier and wetter periods (Andrade et al., 2019; Cabrini et al., 2022).

The Eddy Covariance (EC) technique is a well-established micrometeorological method and the only one through which it is possible to obtain nearly direct, continuous, and non-intrusive measurements of the greenhouse gases fluxes, based on high-frequency measurements of the vertical component of the wind and a scalar of interest such as H_2O, CO_2, and CH_4 (Baldocchi, 2020). Roberti et al. (2024) analyzed the CO_2 fluxes using the EC technique in a livestock area on native pasture in the Pampa biome and showed that the system emits CO_2 during the autumn and winter periods, but there is significant absorption in the spring and summer, making the ecosystem an annual CO_2 sink. However, the amount of CO_2 absorbed annually shows great variability. In that study no technique was used to identify patterns related to climatic phenomena. Here we aim to use wavelet techniques to identify such patterns focused in ENSO phenomenon.

The Continuous Wavelet Transform (CWT) is a powerful tool for capturing and analyzing temporal variations and frequency characteristics that change over time (Segele et al., 2009; Labat, 2010; Juez et al., 2020). It offers adjustable temporal and frequency resolution, facilitating the identification of short-term and high-frequency meteorological patterns that may be obscured in broader, global analyses (Zeri et al., 2020). This makes CWT particularly valuable for visualizing subtle differences in the behavior of environmental variables. Moreover, CWT is effective in detecting nuanced short-term variations, providing a detailed perspective on CO_2 dynamics and ecosystem responses under varying meteorological conditions. Cross Wavelet Transform (XWT) analysis enables an in-depth examination of the covariation between two time series, quantifying both, the magnitude of their shared power, and the phase relationships, over time. This approach is essential for identifying temporal synchronizations between CO_2 fluxes and meteorological variables, revealing how these interactions fluctuate across different timescales. By emphasizing phase relationships and shared power, XWT provides valuable understanding of the interaction dynamics between paired time series. In further investigations a XWT will be applied to determine the behavior of the meteorological variables to the ENSO phenomenon, where significant anticorrelations can be extracted. Therefore, this study uses these techniques to evaluate the influence of meteorological variables during El Niño (EN) and La Niña (LN) periods on CO_2 fluxes, in a natural pasture of the Pampa biome, which is utilized for livestock production in Santa Maria, Rio Grande do Sul, Brazil.

2 METHODOLOGY

2.1 Experimental site

The Santa Maria Experimental Site (SMA) (Figure 1) is located at the following geographic coordinates: latitude: 29° 43'27.502''S and longitude: 53° 45'36.097''W, with an altitude of 88 meters. Encompassing an area of approximately 24 hectares, the site exhibits vegetation characteristic for the Pampa biome. The climate in the region is classified as humid temperate (Cfa) according to the Köppen classification (Kottek et al., 2006). The summers are hot, with temperatures that can reach 40°C in January, while the winters are milder, with temperatures approaching 0°C and the presence of frosts. The typical climatic annual precipitation of 1778 mm is evenly distributed throughout the year.

Regarding the soil in the experimental area, it is classified as Ultisol, according to the FAO classification of (2015), with a composition of 47% sand, 17% clay, and 36% silt (Rubert et al., 2018). The vegetation found at the study site, is classified as a grassland sub-type belonging to the Inland Sub-Montane Grassland (Hasenack et al., 2023). The most abundant grass species in the area are *Axonopus affinis*, *Paspalum notatum*, *Andropogon lateralis*, and *Aristida laevis*, which are evenly distributed throughout the study area (Kuinchtner et al., 2018). This vegetation is used as pasture for beef cattle, and there are no indications that any soil management has been carried out other than for livestock purposes.

Figure 1 – Location of the Santa Maria experimental site in the Pampa biome and flux tower

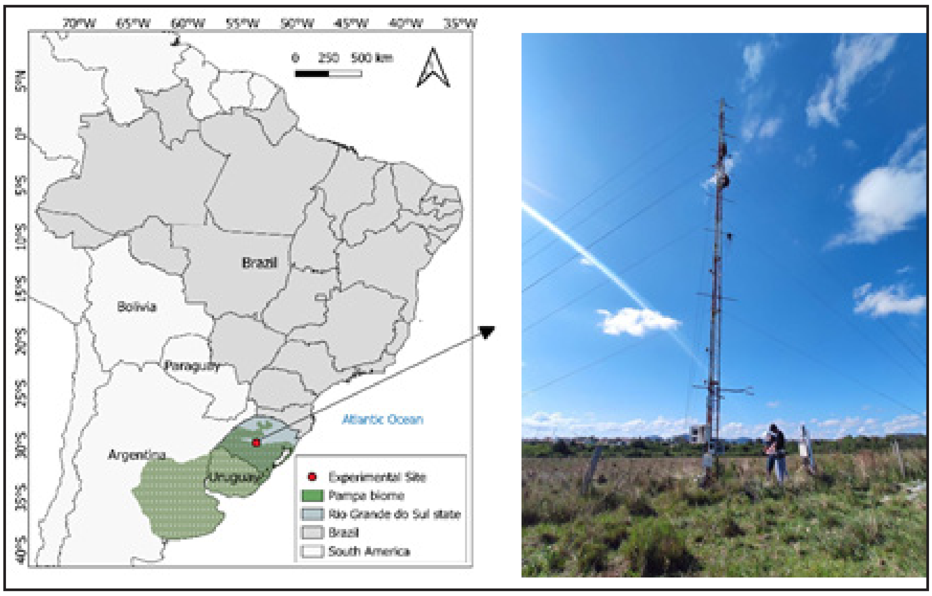

Source: Authors (2024)

2.2 Ocean anomalies associated with El Niño and La Niña

The Table (1) shows the 2015 and 2022 ENSO anomalies. The Warm (El Niño - 2015) and Cool (La Niña - 2022) periods are based on a ± 0.5 °C threshold for the Niño Oceanic Index (ONI) on consecutive 3-month averages of ocean anomalies in the sea surface temperature with respect to the so called Niño 3.4 region (5°N to 5°S, 120° to 170° W), based on 30-year periods updated every 5 years. The 2015 El Niño phenomenon presented positive anomalies of up to 2.6°C of the surface temperature in the tropical Pacific Ocean, indicating an intense El Niño, principally in the second half of the year. La Niña, in the year 2022, presented an average with negative anomalous values indicating a continued influence of this oceanic anomaly, and making them ideal for studying this influence in particular. In this study we will analyses these years to evaluate the influence of EN and LN in the CO2 fluxes in SMA site.

Table 1 – ENSO anomalies during 2015 and 2022

Year	DJF	JFM	FMA	MAM	AMJ	MJJ	JJA	JAS	ASO	SON	OND	NDJ
2015	0.5	0.5	0.5	0.7	0.9	1.2	1.5	1.9	2.2	2.4	2.6	2.6
2022	−1.0	−0.9	−1.0	−1.1	−1.0	−0.9	−0.8	−0.9	−1.0	−1.0	−0.9	−0.8

Source: NOAA

2.3 Instruments and data processing

A flux tower was installed in the middle of the SMA experimental area with the equipment used in this study listed in Table (2). Here, the data collected during 2015 and 2022 were used. The processing of the high-frequency data to estimate CO2 flux, or CO2 net exchange ecosystem (NEE) was performed using the Eddy Covariance technics by the software EddyPro® version 7.0.6 (Li-Cor, Lincoln, Nebraska) into 30-minute averages. The following corrections were applied: double rotation, density correction, attenuation of flux due to instrumental configuration, high-pass filter corrections and low-pass filter correction (Webb et al., 1980; Gash and Culf 1996; Wilczak et al. 2001; Moncrieff et al. 2004).

Table 2 – Flux tower equipment in SMA experimental site

Variable (data frequency)	Position (m)	Sensor model (Manufacturer)
Wind speed components (10 Hz)	3	Wind Master Pro (Gill instruments, Hampshire, UK)
CO2/H2O concentration (10 Hz)*	3	LI7500 (LI-COR Inc., Lincoln, NE, USA)
CO2/H20 concentration (10 Hz)**	3	IRGASON (Campbell Scientific Inc., Logan, UT, USA)
Air temperature and Relative Humidity (1 Hz)	3	HMP155 (Vailasala, Finland)
Precipitation (1 Hz)	6	TR525USW (Texas electronics, Dallas, TX, USA)
Global Solar Radiation (1 Hz)	3	CMP3 (Kipp and Zonen, Delft, The Netherlands)
Soil Temperature (1 Hz)	-0.05	T108 (Campbell Scientific Inc., Logan, UT, USA)
Soil Water Content (1 Hz)	-0.1	CS 616(Campbell Scientific Inc., Logan, UT, USA)

* in 2015; ** in 2022
Source: Authors (2024)

The EddyPro® software provides a quality flag for the fluxes based on the principles of atmospheric stability and well-developed turbulence (Foken et al., 2004): Flag “0” indicates the fluxes as good quality, while Flag “1” marks moderate quality fluxes, whereas Flag “2” indicates low-quality fluxes and are therefore discarded. The remaining fluxes undergo a filtering process that removes non-physical values, based on adapted equations from Béziat et al. (2009). Lastly, the friction velocity (u*) filter was applied, following the guidelines outlined in accordance with Papale et al. (2006). The results of this procedures was 46.66% of the NEE remaining data, which corroborates to the EC technique literature (Papale et al., 2006). The Reddyproc package (Max Planck Institute for Biogeochemistry, Germany. https://www.bgc-jena.mpg.de/REddyProc/ui/REddyProc.php) was used to fill the gaps, following Wutzler et al. (2018) methodology.

The gaps in meteorological data (air temperature - Tair, Solar Global Radiation - Rg and Relative Humidity - RH) were filled using official measurements from the Brazilian Meteorological Institute (INMET) taken from the WMO station 86977, located approximately 4 km from the SMA site. The remaining gaps were corrected using hourly data from the ERA5 reanalysis, with a spatial resolution of 0.25°, obtained from the Copernicus Climate Change Service (C3S) Climate Data Store (CDS) (Hersbach et al., 2018). The INMET station database was also used to obtain climatological data (30-year average, 1991–2020).

2.4 CWT and XWT Wavelet

The Continuous Wavelet Transform (CWT) is a tool for analyzing localized intermittent oscillations in a time series. The step-by-step procedure and fundamental concepts of the CWT are presented in Morlet (1983). The theoretical framework for wavelet analysis is detailed in Daubechies (1992), following the guidelines outlined by Torrence and Compo (1998). It is possible to construct the Cross-Wavelet Transform (XWT) from two CWTs, which will expose their common power and relative phase in time-frequency space (Torrence and Compo, 1998). The XWT analysis is conducted based on the methodologies proposed by Grinsted et al. (2004), utilizing MATLAB as the computational platform along with the toolbox developed by the same authors. The tools used int this work are available on https://grinsted.github.io/wavelet-coherence/

3 RESULTS

3.1 Environmental variables in 2015 and 2022

Figure 2 presents the monthly averages of meteorological variables (Precipitation, Prec; Air temperature, Tair; Relative Humidity, RH; Soil Water Content, SWC; Solar radiation, Rg and Soil temperature, Tsoil) for 2015 and 2022 and the climatological average of Prec and Tair at the SMA site. The precipitation in 2015 remained close to the climatological average from January to September, but was significantly higher in October and December. In 2022, the year started with precipitation below the climate average, but this was compensated by high precipitation in the following months. However, from August onwards the precipitation stayed below the climatological average. During the period from March to September 2015, Tair was increased with an average of 1°C above compared to the climatological average, but it remained below the average from November to the rest of the year. In 2022, influenced by La Niña, predominantly below-average values were observed, with the exception of January, February, July, and the last two months of the year, which showed a period of greater ENSO influence in the region. In 2015, relative humidity (RH) and soil water content (SWC) were lower. This can be explained by the phenomenon of the 'Vento Norte' (Portuguese for north wind), which affected the region, bringing hot and dry wind (Stefanello et al., 2020). The solar radiation at the SMA site was similar between February and August during the years 2015 and 2022, with a similar behavior in SWC, but Rg declined to the end of 2015 probably due to a period of heavy rainfall, and extensive cloud cover, which also kept the SWC high in this period. In 2022, we observed higher Tsoil values compared to 2015, with the exception of May, June, and August.

Figure 2 – Monthly meteorological variables for the 2015 and 2022 and climatological averages for SMA site

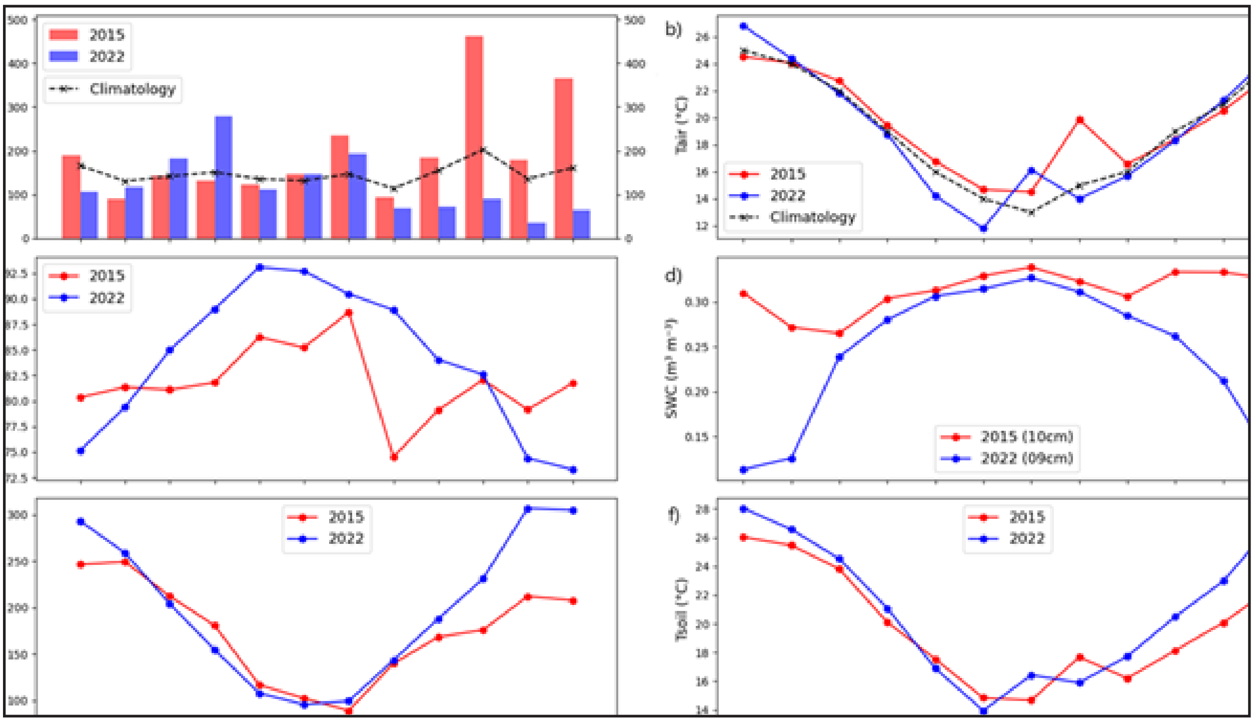

Source: Authors (2024)

3.2 CO2 flux

Figure 3 shows the half-hour and monthly average of CO_2 NEE over the years 2015 and 2022 at the SMA site. Positive values indicate CO_2 emissions by the ecosystem, while negative values indicate absorption. In general, positive NEE occurs at night, reflecting only the respiration processes of the ecosystem that releases CO_2. Negative NEE indicates that photosynthesis is surpassing ecosystem respiration, resulting in CO_2 absorption. A seasonal pattern is observed in both years, with higher absorption and emission in spring and summer (September to February). During autumn and winter (March to August), the amount of absorption decreases more rapidly than emission processes. In 2015, the Pampa biome showed a greater capacity for CO_2 absorption in the periods from January to April and from October to December, compared to 2022.

In 2022, the difference between emission and absorption was smaller than in 2015.

Figure 3 – Half-hour and monthly average of CO2 NEE in 2015 and 2022 for SMA site

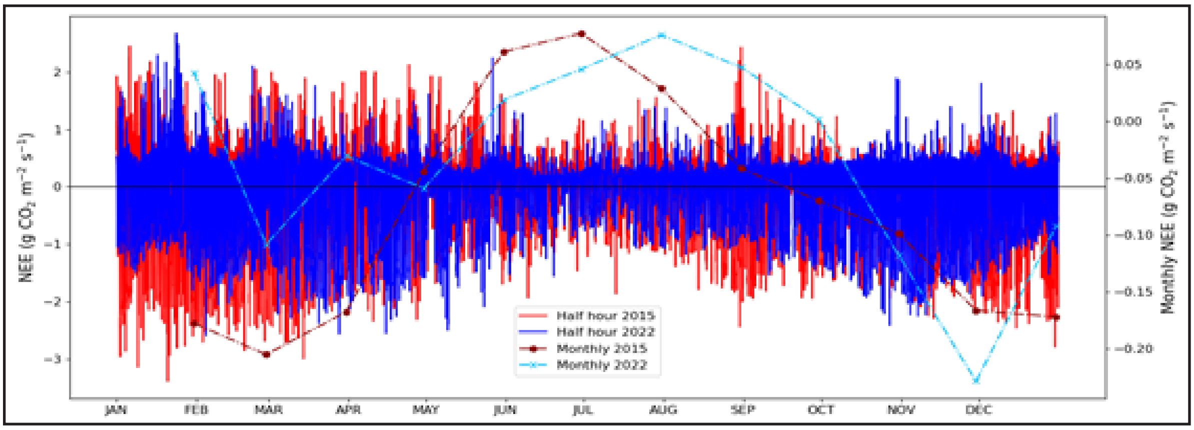

Source: Authors (2024)

3.3 Continuous Wavelet Transform analysis (CWT)

In this study, half hour dataset for NEE, Prec, Rg and Tair, were analyzed for each year (2015 and 2022) using the CWT, as presented in Figure (4). To interpret these plots, it is essential to consider the signal amplitude. The bar on the right in Figure (4) indicates the magnitude of the signal, i.e., the variance of the time series analyzed at different frequencies. The color bar (from blue to yellow) indicates the intensity of the oscillation on a logarithmic scale to the base 2. For example, a value of -4 (blue) on the color bar represents 2-4 = 1/16, where a value of 4 (orange) is 24 = 16. The black contour line, commonly referred to as the cone of influence, shows the 95% significance level (above), while what is below represents only 5%. Therefore, in Figure (4 a and b), the higher powers (yellow areas) represent periods when the Pampa biome acted as a CO_2 sink, while the blue areas in the spectrum indicate periods dominated by CO_2 emission. For example, during the months from July to September, there is a higher emission pattern in both years, which is associated with winter in those months (Figure 3) (Mergen, 2022). This period is historically wetter and has less radiation availability for photosynthesis. However, there is an amount of absorption during

2022, between the end of July and the beginning of August, reflecting the occurrence of a "veranico" (a short period of hot weather) caused by the persistence of the "North Wind" phenomenon in the region during that year.

The precipitation presented in the bar chart of Figure 2, is also analyzed using the CWT, as shown in Figure 4 (c and d). This approach allows for a more detailed understanding of the temporal variation of Prec over the months. The results show that the rainfall in 2015 was dominant mainly in spring and summer. During these months, the rainfall significantly contributed to the increase in soil moisture, and consequently to the productivity of the ecosystem. In contrast, the analysis for 2022, influenced by the La Niña phenomenon, shows that rainfall was below the average, adversely affecting vegetation and the CO_2 absorption capacity of the biome. The CWT technique shows additionally that the winters of 2015 and 2022 were characterized by humidity, indicating that even in the years of lower precipitation, the water availability was sufficient to sustain vegetation during these critical months.

For Rg, Figures (4e and f) show the influence of the ENSO phenomenon on this variable. As discussed in relation to Prec, Rg is also more affected during the spring and summer periods (September to February) probably due to increased cloud cover during the rainy seasons, which reduces solar radiation levels. On the other hand, during periods of low Prec cloud cover decreases resulting in higher Rg values. The air temperature (Tair) variable showed higher power during the winter of 2015 compared to the winter of 2022. In 2022, a decrease in power was observed, along with a greater number of gaps, shown evidently the 16-day periodicity. Overall, the analysis of Tair using the CWT technique showed similar results in both studied periods with small variation (Figure 4g and 4h).

The analysis presented here is similar to presented by Qin et al. (2008), Hong and Kim (2010), Vadrevu and Choi (2011), Rocha (2018), Göckede et al. (2019), and Zeri et al. (2020). They also used the wavelet technique for visualizing flux data, achieving results across different temporal and spatial scales, which enables the identification of patterns in the behavior of these fluxes. In this study, the CWT analysis for EL and LN shows differences in precipitation on a scale of 16 to 32 days, while other variables do not present striking differences.

Figure 4 – CWT and global wavelet power spectrum for NEE, Prec, Rg and Tair for the years 2015 (EN) and 2022 (LN)

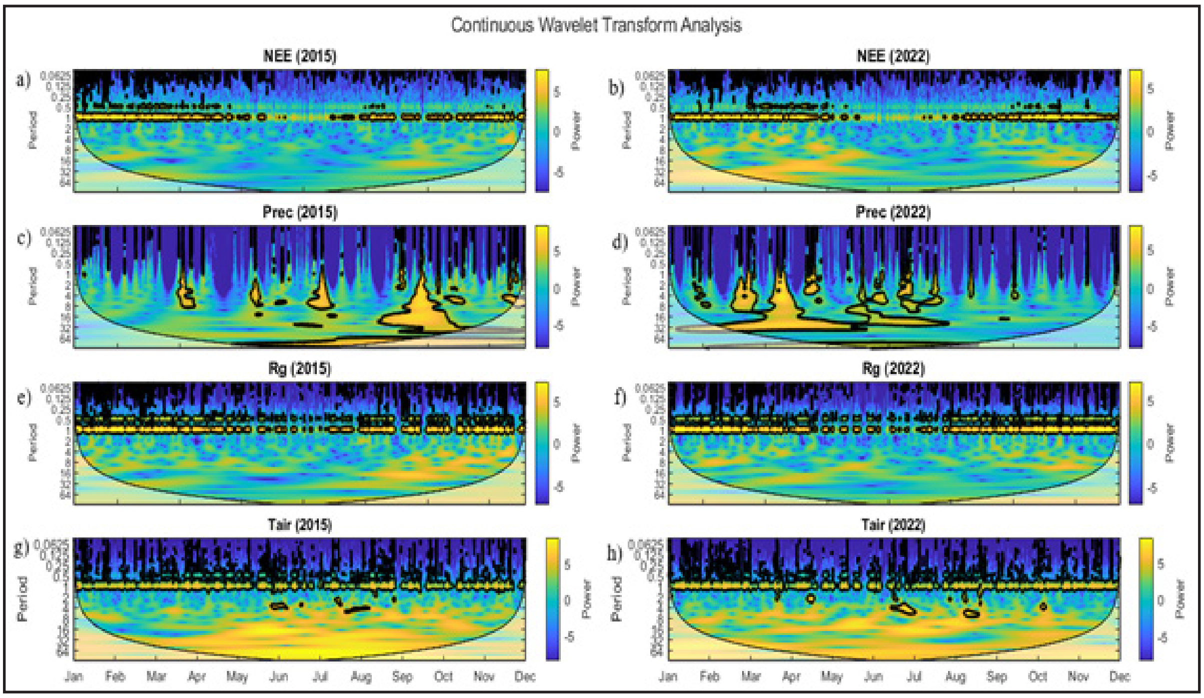

Source: Authors (2024)

3.4 Cross Wavelet Transform analysis (XWT)

The XWT analysis shows the relative phase relationship between the two time series, and the phase arrows play a crucial role in interpreting the results. In Figure 5, the XWT between NEE and Prec, Rg, and Tair are presented. The direction of the arrows can be interpreted as a lead or lag between the signals. For instance, an arrow pointing to the right indicates that the series are in phase (directly proportional), while an arrow pointing to the left suggests an anti-phase relationship (inverse). Additionally, arrows pointing up (lead) or down (lag) indicate that one series is leading the other by a phase of 90°. In Figure (5a and b) the arrows pointing to the right, indicating a direct proportional relationship between NEE and Prec. This correlation suggests that rainfall increases the physiological activity of plants, resulting in greater carbon emission and absorption, especially in the warmer months of the analyzed years. Precipitation provides adequate soil moisture favoring photosynthesis and plant respiration. Thus, periods of higher precipitation can lead to a significant increase in the plants' capacity to absorb CO_2, reflecting a positive dynamic between NEE and Prec.

The relationship between NEE and Rg shows that variations in Rg precede fluctuations in carbon emission (Figure 5c and d). This behavior indicates that the increase or decrease of Rg levels exerts direct control over NEE, determining subsequent responses in the ecosystem's carbon balance. Arrows pointing to the left, show evidence for this relationship, suggesting that solar radiation regulates the physiological processes that influence NEE, modulating both CO_2 absorption and emission by the ecosystem.

The NEE and Tair relationship (Figures 5e and 5f) represents a response to the relationship between NEE and Prec and NEE and Rg. On cloudy and rainy days, air temperature exhibits low thermal amplitude, while on sunny days with low cloud cover, air temperature shows greater variation, especially in the spring and summer months. Figure 5e (corresponding to the year 2015) shows that in some times of the year, especially in the warmer months (summer and late spring), the arrows indicate a direct relationship between NEE and Tair (with arrows pointing to the right). This indicates that during these periods an increase in the air temperature tends to be associated with greater ecosystem activity in terms of CO_2 emission or absorption. In Figure 5e, referring to the year 2015. It is noted, in some times of the year, especially in the warmer months (summer and late spring), the arrows point to the right, indicating a direct relationship between NEE and Tair. This suggests that during these periods, an increase in air temperature tends to be associated with intensified ecosystem activities, both in CO_2 emission and absorption. On the other hand, in Figure 5f, which shows the relationship between NEE and Tair in 2022, a similar behavior to that of 2015 is observed, but with differentiated coherence patterns throughout the year and more discrete variability in certain periods. At some points, the arrows point to the right, indicating a direct proportional phase between NEE and Tair, while in other periods the arrows point to the left, suggesting an inverse relationship. This pattern in 2022 may be related to distinct climatic conditions, such as the La Niña event.

From XWT analysis, unlike other techniques or conventional graphs, it is possible to observe both the direct and inverse relationships between the variables and their responses, whether anticipated or delayed. Moreover, the analysis allows identifying the periodicity and periods of greater coherence in the relationship between the time series. Here, we identified the main differences between the EL and LA phenomena on a time scale between 16 to 32 days in the relationship of NEE and Prec, occurring in spring for EL and summer/autumn in LN.

Figure 5 – Cross Wavelet Transform (XWT) for NEE, Prec, Rg and Tair, for the years 2015 (EN) and 2022 (LN)

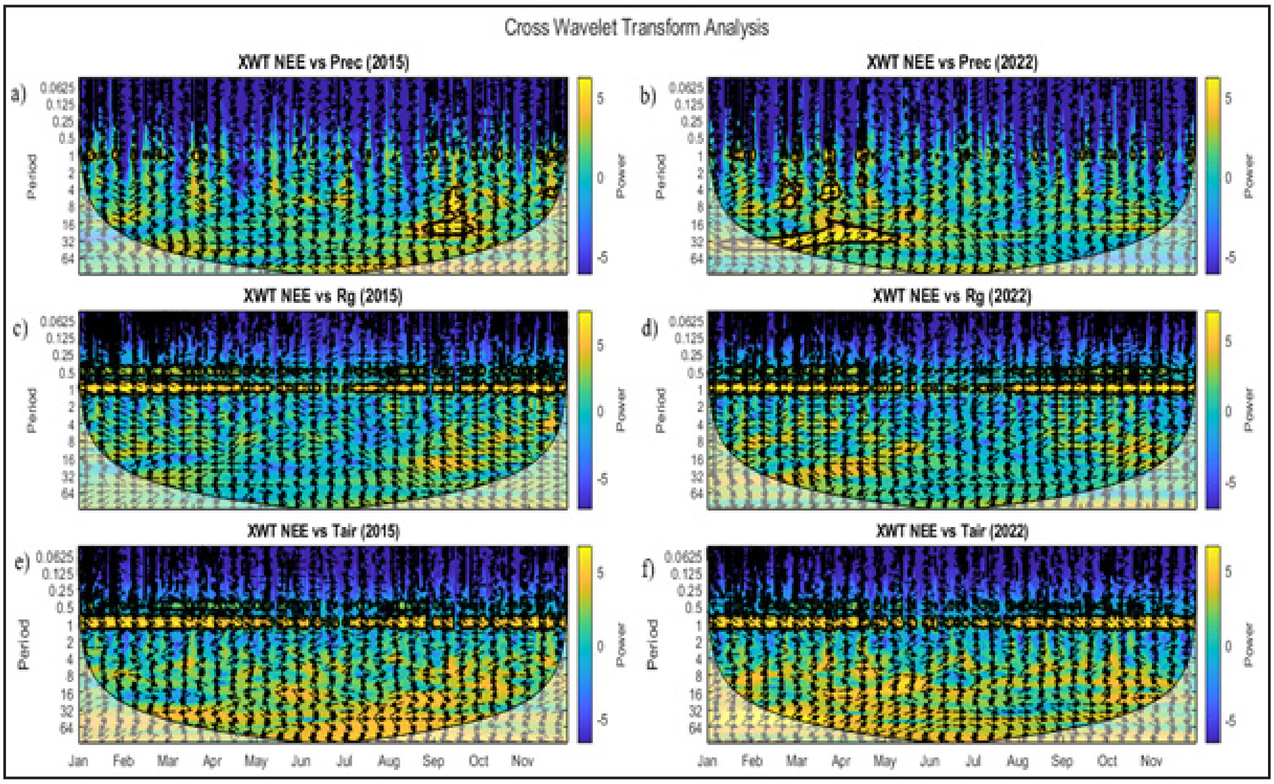

Source: Authors (2024)

4 CONCLUSIONS

The application of the continuous wavelet transform was shown for the meteorological data and CO2 flux obtained in a flux tower in Santa Maria experimental site (SMA) in the Brazilian pampa biome. It was shown that the wavelet transform from year 2015 (EN) in comparison to year 2022 (LN), interesting finite temporal occurring non-stationary multi-frequency processes from meteorological variables can be deduced. This shows the high potential of this method in determining relationships within this variables, specially the monitorization of the CO2 emissions and absorption processes during the year of the ENSO phenomena. The cross wavelet transform for analyzing two time series together gave refined insights into the correlation of these variables. It permits identify important relationships, essential to develop modeling to estimate the CO2 flux concerning meteorological trends.

ACKNOWLEDGEMENTS

This study has been partially supported by Conselho Nacional de Desenvolvimento Científico e Tecnológico (CNPq), Fundação de Amparo à pesquisa do Estado do Rio Grande do Sul (FAPERGS), by Coordenação de Aperfeiçoamento de Pessoal de Nível Superior-Brasil (CAPES). We acknowledge the organizers of IX Encontro Sul Brasileiro de Meteorologia.

REFERENCES

ANDRADE, B. O. et al., Classification of South Brazilian grasslands: Implications for conservation. **Applied Vegetation Science**, v. 22, n. 1, p. 168-184, 2019.

BALDOCCHI, D. D., How eddy covariance flux measurements have contributed to our understanding of Global Change Biology. **Global change biology**, v. 26, n. 1, p. 242-260, 2020.

BÉZIAT, P.; CESCHIA, E.; DEDIEU, G. Carbon balance of a three crop succession over two cropland sites in South West France. **Agricultural and Forest Meteorology**, v. 149, n. 10, p. 1628-1645, 2009.

BOLDRINI, I. L., **Bioma Pampa: diversidade florística e fisionômica.** Editora Pallotti, 2010.

CABRINI, S.; COLUSSI, J.; SCHNITKEY, G., Third Consecutive La Niña? What to Expect from Soybean Yields in the United States, Brazil and Argentina. **farmdoc daily**, v. 12, n. 75, 2022.

DAUBECHIES, I., Ten lectures on wavelets: Society for Industrial and Applied Mathematics. **PA, USA,** 1992.

FOKEN, T. et al. Post-field data quality control. In: **Handbook of micrometeorology: a guide for surface flux measurement and analysis.** Dordrecht: Springer Netherlands, p. 181-208, 2004.

GASH, J. H. C., CULF, A. D. Applying a linear detrend to eddy correlation data in realtime. **Boundary-Layer Meteorology**, v. 79, n. 3, p. 301-306, 1996.

GÖCKEDE, M., KITTLER, F., SCHALLER, C., Quantifying the impact of emission outbursts and non-stationary flow on eddy-covariance CH 4 flux measurements using wavelet techniques. **Biogeosciences**, v. 16, n. 16, p. 3113-3131, 2019.

GRINSTED, A., MOORE, J. C., JEVREJEVA, S., Application of the cross wavelet transform and wavelet coherence to geophysical time series. **Nonlinear processes in geophysics**, v. 11, n. 5/6, p. 561-566, 2004.

HASENACK, H. et al. Biophysical delineation of grassland ecological systems in the State of Rio Grande do Sul, Southern Brazil. **Iheringia, Série Botânica**., v. 78, 2023.

HERSBACH, H. et al. ERA5 hourly data on single levels from 1959 to present. Copernicus Climate Change Service (C3S) Climate Data Store (CDS). **H. Hersbach, Bell, B., Berrisford, P., Biavati, G., Horányi, A., Muñoz Sabater, J., Nicolas, J., Peubey, C., Radu, R., Rozum, I., Schepers, D., Simmons, A., Soci, C., Dee, D., Thépaut, JN.(Ed.)**, 2018.

HERZOG, H., ELIASSON, B., KAARSTAD, O., Capturing greenhouse gases. **Scientific American**, v. 282, n. 2, p. 72-79, 2000.

HONG, J., KIM, J., Impact of the Asian monsoon climate on ecosystem carbon and water exchanges: a wavelet analysis and its ecosystem modeling implications. **Global change biology**, v. 17, n. 5, p. 1900-1916, 2011.

JUEZ, C. et al. Wavelet analysis of hydro-climatic time-series and vegetation trends of the Upper Aragón catchment (Central Spanish Pyrenees). **Journal of Hydrology**, v. 614, p. 128584, 2022.

KOTTEK, M.; GRIESER, J.; BECK, C.; RUDOLF, B.; RUBEL, F. World Map of the Köppen-Geiger climate classification updated. **Meteorol. Z**, v. 15, p. 259–263. 2006.

KUINCHTNER, B. C. et al. Performance and feed intake of beef heifers on rotational grazing of natural grassland receiving protein and energy supplement in cool season. **Ciência Rural**, v. 48, n. 4, p. e20170563, 2018.

LABAT, D. Cross wavelet analyses of annual continental freshwater discharge and selected climate indices. **Journal of Hydrology**, v. 385, n. 1-4, p. 269-278, 2010.

LOBATO, R. R. C, Variabilidade dos fluxos de energia e evapotranspiração sob influência do ENOS no Bioma Pampa brasileira. Dissertação de Mestrado, Universidade Federal de Santa Maria. 2022.

MERGEN, A., Variabilidade interanual dos fluxos de CO2 em uma pastagem natural no bioma Pampa brasileiro. Dissertação de Mestrado, Universidade Federal de Santa Maria. 2022.

MONCRIEFF, J. B. et al. Averaging, detrending, and filtering of eddy covariance time series. In: **Handbook of micrometeorology: A guide for surface flux measurement and analysis.** Dordrecht: Springer Netherlands, p. 7-31, 2004.

MORLET, J. Sampling theory and wave propagation. In: **Issues in acoustic Signal—image processing and recognition.** Springer Berlin Heidelberg, p. 233-261, 1983.

PAPALE, D. et al. Towards a standardized processing of Net Ecosystem Exchange measured with eddy covariance technique: algorithms and uncertainty estimation. **Biogeosciences**, v. 3, n. 4, p. 571-583, 2006.

POPP, A.; LOTZE-CAMPEN, H.; BODIRSKY, B., Food consumption, diet shifts and associated non-CO2 greenhouse gases from agricultural production. **Global environmental change**, v. 20, n. 3, p. 451-462, 2010.

QIN, Z. et al. Characterization of CO2 and water vapor fluxes in a summer maize field with wavelet analysis. **Ecological Informatics**, v. 3, n. 6, p. 397-409, 2008.

REICHERT, H.; SCHUMACHER, G., A pecuária no rio grande do sul: a origem, a evolução recente dos rebanhos e a produção de leite. Departamento de Ciências Econômicas da Universidade Federal de Santa Maria. Recuperado de http://cdn. fee. tche. br/eeg/6/mesa13/A_Pecuaria_no_RS-A_origem_Evolucao_Recente_dos_Rebanhos_e_a_Producao_de_Leite. pdf, 2015.

ROBERTI, D. R. et al. Sustainability in Natural Grassland in the Brazilian Pampa Biome: Livestock Production with CO2 Absorption. **Sustainability**, v. 16, n. 9, p. 3672, 2024.

RUBERT, G. C. et al. Evapotranspiration of the Brazilian Pampa biome: Seasonality and influential factors. **Water**, v. 10, n. 12, p. 1864, 2018.

ROESCH, L. F. W., et al. The Brazilian Pampa: a fragile biome. **Diversity**, v. 1, n. 2, p. 182-198, 2009.

ROCHA, A. A. F. Espectro cruzado e coerência wavelet: um estudo de variáveis micrometeorológicas em frações urbanas na cidade de Cuiabá, MT. Tese de doutorado, Universidade Federal de Mato Grosso, Cuiabá. 2018.

SCHOSSLER, V. et al. Precipitation anomalies in the Brazilian southern coast related to the SAM and ENSO climate variability modes. **RBRH**, v. 23, p. e14, 2018.

SEGELE, Z. T.; LAMB, P. J.; LESLIE, L. M. Seasonal-to-interannual variability of Ethiopia/horn of Africa monsoon. Part I: associations of wavelet-filtered large-scale atmospheric circulation and global sea surface temperature. **Journal of Climate**, v. 22, n. 12, p. 3396-3421, 2009.

STEFANELLO, M. et al. A micrometeorological analysis of the Vento Norte phenomenon in southern Brazil. **Boundary-Layer Meteorology**, v. 176, p. 415-439, 2020.

TORRENCE, Christopher; COMPO, Gilbert P. A practical guide to wavelet analysis. **Bulletin of the American Meteorological society**, v. 79, n. 1, p. 61-78, 1998.

VADREVU, K. P., CHOI, Y., Wavelet analysis of airborne CO2 measurements and related meteorological parameters over heterogeneous landscapes. **Atmospheric Research**, v. 102, n. 1-2, p. 77-90, 2011.

WEBB, E. K, PEARMAN, G. I., LEUNING, R., Correction of flux measurements for density effects due to heat and water vapour transfer. **Quarterly Journal of the Royal Meteorological Society**, v. 106, n. 447, p. 85-100, 1980.

WILCZAK, J. M.; ONCLEY, S. P.; STAGE, S. A. Sonic anemometer tilt correction algorithms. **Boundary-layer meteorology**, v. 99, p. 127-150, 2001.

WUTZLER, T. et al. Basic and extensible post-processing of eddy covariance flux data with REddyProc. **Biogeosciences**, v. 15, n. 16, p. 5015-5030, 2018.

ZERI, M. et al. Nitrous oxide fluxes over establishing biofuel crops: Characterization of temporal variability using the cross-wavelet analysis. **GCB Bioenergy**, v. 12, n. 9, p. 756-770, 2020.

Authorship contributions

1 – João Antonio Voltz da Silva

Universidade Federal de Santa Maria. Meteorologia, Graduando em Meteorologia
https://orcid.org/0009-0004-9108-3805 • joaovoltz17@gmail.com
Data curation, Writing – review & editing, Writing – original draft

2 – Débora Regina Roberti

Universidade Federal de Santa Maria. Física, Doutora em Física
https://orcid.org/0000-0002-3902-0952 • debora@ufsm.br
Supervision

3 – Benno August Ludwig Bodmann

Universidade Federal de Santa Maria. Físico, Doutor em Física
https://orcid.org/0009-0006-0358-8358 • benno.bodmann@gmx.de
Writing – original draft, Writing – review & editing

4 – Richard Reno da Costa Lobato

Universidade Federal de Santa Maria. Meteorologista, Mestre em Meteorologia
https://orcid.org/0000-0003-3787-6738 • richardlobato7@gmail.com
Writing – original draft

5 – Alecsander Mergen

Universidade Federal de Santa Maria. Físico, Mestre em Física
https://orcid.org/0000-0001-7126-8694 • alecsandermergen@gmail.com
Data curation, Writing – original draft, Writing – review & editing

How to quote this article

Silva, J. A. V., Bodman, B. A., Roberti, D. R., Lobato, R. R. C., & Mergen, A. (2025). Wavelet analysis applied to greenhouse gas exchange in livestock. *Ciência e Natura*, Santa Maria, v. 47, n. esp. 3, e84042. DOI: https://doi.org/10.5902/217946084042. Disponível em: https://doi.org/10.5902/2179460X84042.